A new adaptive nonuniformity correction algorithm for infrared line scanner based on neural networks

Jing Sui (隋 婧), Liquan Dong (董立泉), Weiqi Jin (金伟其), and Yayuan Zhang (张雅元)

Laboratory of Infrared Technology, School of Information Science and Technology, Beijing Institute of Technology, Beijing 100081

Received August 10, 2006

The striping pattern nonuniformity of the infrared line scanner (IRLS) severely limits the system performance. An adaptive nonuniformity correction (NUC) algorithm for IRLS using neural network is proposed. It uses a one-dimensional median filter to generate ideal output of network and can complete NUC by a single frame with a high correction level. Applications to both simulated and real infrared images show that the algorithm can obtain a satisfactory result with low complexity, no need of scene diversity or global motion between consecutive frames. It has the potential to realize real-time hardware-based applications.

OCIS codes: 040.3060, 100.2550, 100.2980, 200.4260.

Infrared line scanner (IRLS) is widely used for civil and space imaging applications. It suffers from a common problem, fixed pattern noise (FPN) or spatial nonuniformity, which results from the different responses of each sensor to the uniform irradiance. For IRLS, FPN is usually manifested as horizontal stripes. It is temporally constant and drifts slowly with the external factors. Despite recent rapid advances in nonuniformity correction (NUC) technology[1−4], the striping nonuniformity for IRLS remains a serious problem. Though many NUC algorithms can have, to some degree, a better effect in correcting staring type focal plane arrays (FPAs), but they are not readily applied to the scanning type FPA. Here we propose an adaptive neural network NUC algorithm for IRLS. It does not need any motion existing between frames and can complete nonuniformity compensation in only a single frame. Assuming the NUC parameters of each sensor remain constant in a certain block of frames, and random drift exists between blocks, then the algorithm may be further simplified by using the correction results of a single frame instead of a block. So the commercial potential of this algorithm is huge.

The response of detector is modeled linearly. Suppose each pixel in the image is a neuron, and each neuron has a weight and a bias. For IRLS, the weights and biases in each row are all the same, namely, $g(i,j) = g(i)$ and $o(i,j) = o(i)$, so a commonly used linear model for the (i,j)th FPA-sensor output $y(i,j)$ is given by

$$\hat{x}(i,j) = \hat{g}(i) \cdot y(i,j) + \hat{o}(i), \tag{1}$$

where, $i = 1, 2, \cdots, M$ and $j = 1, 2, \cdots, N$. $x(i,j)$ is the irradiance actually received by each sensor. $g(i)$ and $o(i)$ represent gain and offset of the detector. If the parameters are adaptive, the model in Eq. (1) can be considered as the simplest neural network (NNT) structure. When the sensor readout data $y(i,j)$ inputs to the neuron, $\hat{x}(i,j)$, $\hat{g}(i)$ and $\hat{o}(i)$ are the corresponding estimated output values.

In traditional NNT algorithms[5,6], $\hat{g}(i,j)$ and $\hat{o}(i,j)$ must be renewed frame by frame by using the steepest descent linear regression[1−4] and scene variation between frames is needed. But when the traditional methods are applied to sequence produced by IRLS, they cannot remove the horizontal stripes effectively. Furthermore, if the difference between neighboring frames is not sufficient, the renewing process of correction parameters may be degenerated, or severe ghosting artifacts will be produced. So the sufficient global motion between neighboring frames is required.

Considering all the above limitations, an adaptive NNT algorithm aiming at scanning type IRLS is proposed. For a frame obtained from IRLS of size $M \times N$, only M detectors (neurons) need correcting, hence the numbers of gains and offsets corresponding to the IRLS are M. For every row, each neuron corresponds to N outputs, or N values recorded.

In the improved method, $\hat{g}(i)$ and $\hat{o}(i)$ must be updated column by column using linear regression to obtain a good estimation for the real infrared data.

However, the learning process based on steepest descent model is not robust enough, and the production of ghosting artifacts cannot be effectively prevented, which is a problem presented in most scene-based NUC techniques. To improve the parameter update process, some optimization methods[6] are adopted, including momentum, regularization and adaptive learning rate.

The three optimizations have their own advantages respectively. Specifically, the regularization factor r is only added to the gain updating, forcing all the gain values in the same column to have a unitary mean, and accelerating the convergence rate. The use of momentum can improve the stability of the algorithm by preventing the local minima problem and suppressing the production of ghosting. Furthermore, the adaptive learning rate $\eta(i,j)$ is defined to be inversely proportional to $\sigma_y^2(i,j)$ which is the local spatial square variance of the input image $y(i,j)$. It can speed up the convergence greatly and control the production of artifacts. Hence after optimizing strategy, the equation of parameter learning process can be improved as

$$\begin{aligned}\hat{g}_i(j+1) = \hat{g}_i(j) - \eta(i,j) \cdot E(i,j) \cdot y(i,j) \\ +\alpha \cdot [\hat{g}_i(j) - \hat{g}_i(j-1)] + r_j,\end{aligned} \tag{2}$$

1671-7694/2007/020074-03

$$\hat{o}_i(j+1) = \hat{o}_i(j) - \eta(i,j) \cdot E(i,j) + \alpha \cdot [\hat{o}_i(j) - \hat{o}_i(j-1)], \quad (3)$$

$$r_j = \lambda \cdot [1 - \frac{1}{M}\sum_{i=1}^{M} g_i(j)], \quad \eta(i,j) = K/[1+\sigma_y^2(i,j)], \quad (4)$$

where λ, α and K (the maximum learning rate allowed) are all constants. Note that η of each frame can be computed together previously as *priori*. The initial values of parameter estimation are $g(i) = 1$ and $o(i) = 0$. $E(i,j)$ is the error function, which is defined as the difference between the estimated output $\hat{x}(i,j)$ and the desired target value $T(i,j)$,

$$E(i,j) = \hat{x}(i,j) - T(i,j). \quad (5)$$

It is notable that the network expected output $T(i,j)$ is not the mean of four nearest neighboring estimated outputs, but a filtered result got from a one-dimensional (1D) median filter which is perpendicular to the direction of horizontal stripes. The reason to choose median filter is that it can smooth off the striation waves, and force the steep gradient along the column to become softer. Especially, the optimal length of filter window should be determined by testing the image quality of the corrected results with different lengths of median filter.

Since the correction is completed in one frame, there are no specific requirements for scene variation of the neighboring frames, thus relaxing the limitations and facilitating its realization in actual hardware.

In order to test the algorithm performance, artificial nonuniformity was introduced in the simulated images by varying the variance of the weights and biases as $\sigma^2_{\text{weight}} = 0.01$ and $\sigma^2_{\text{bias}} = 0.05$. The means of weights and biases are 1 and 0 respectively, and both are of Gaussian random distribution. Every pixel value in the same row multiplies same weight then same bias is plus, thus noise in pattern of horizontal stripes is added to the clear infrared (IR) image.

To study the performance of the proposed method in the mean square error sense, the peak signal-to-noise ratio (PSNR) is defined as

$$\text{RMSE} = \sqrt{\frac{1}{MN}\sum_{i,j}(I_{ij} - \hat{I}_{ij})^2},$$

$$\text{PSNR} = 20 \cdot \log_{10}(\frac{2^b}{\text{RMSE}}), \quad (6)$$

where I_{ij} and $\hat{I}_{ij}$ represent the (ij)th pixel of the clean infrared image and the corrected image respectively, i is the row index of image ranging from 1 to M. The unit for PSNR is dB, larger value for the PSNR indicates higher image quality. The image size is $M \times N$ pixels, and b represents the number of bits per pixel in the image, which in this case is 8.

According to the learning process defined in Eqs. (2)—(5), we have tested the impact of the expected outputs produced by different lengths of median filter windows on PSNR. Here we choose $\lambda = 0.9$, $\alpha = 0.9$ and use a 3×3 window size to compute the local variance $\sigma_y^2(i,j)$, we choose this window size because of its efficiency and good effect[6].

First we need test the optimal length of median filter. Seven lengths of median filter window, i.e. 3×1, 5×1, $\cdots$, 15×1, were applied to the corrupted image and PSNR value of each correction result was computed, as shown in Fig. 1. It is clear that the use of 7×1 window achieves the best performance. Neither too big nor too small window size is satisfactory. By too small window, the smoothing effect is insufficient, while by too big window, the smoothing effect is remarkable, but the details are blurred. Hence the optimal length of window should be determined by comparison of the performance criteria. For a fixed IRLS, the mode of striation is also fixed; once the optimal median filter window is determined, it can be stored and used permanently without change.

Then the correction parameters are evaluated column by column as Eqs. (2)—(5) and result in the gain and offset estimate matrix. Theoretically, the matrix values along rows should be equal, since they are generated by the same detector's output, however, they are not identical in fact. The final compensator should be the average of the estimates along one row, because this can significantly enhance the NUC algorithm's performance compared with directly applying the estimate matrix to the frame.

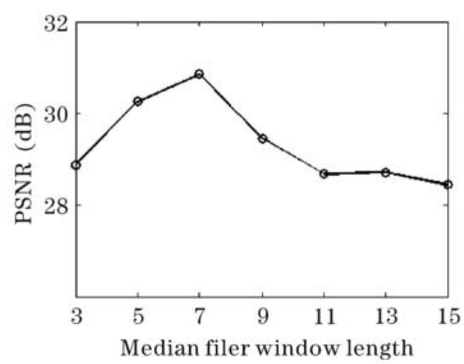

Fig. 1. Impact of median filter length for NUC performance.

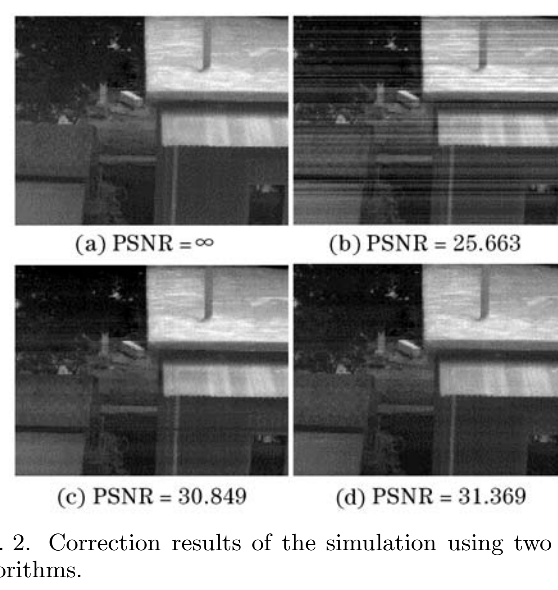

Fig. 2. Correction results of the simulation using two NNT algorithms.

In Fig. 2, the capability of the algorithm in removing nonuniformity is presented, where Fig. 2(a) is the true clean infrared (IR) data, Fig. 2(b) is its corruption with artificial noise. The amount of remnant horizontal artifacts appears noticeable in Fig. 2(c) using traditional NUC method, and Fig. 2(d) shows the corrected result by the improved NNT method, with a better correction level. Their corresponding PSNR values are listed below the diagrams. Usually PSNR value will increase 3—6 after correction.

To test its correction capability, the adaptive NNT algorithm is also applied to real IR data captured with IRLS. We use only one frame captured by a 320 × 240 uncooled scanning type IRLS for correction. In order to obtain best result by using the algorithm, the first thing to do is to determine the optimal median filter window. In real IR data, it is impossible to apply PSNR. So we determine the window by another criterion, the roughness parameter ρ, which is defined as

$$\rho(I) = \frac{\|I_{\mathrm{col}}\|_1 + \|I_{\mathrm{row}}\|_1}{\|I\|_1}, \quad (7)$$

where I is the image matrix, I_{row}, I_{col} represent the difference matrix along rows and columns respectively. $\|\|_1$ is the l_1 norm of I. Its computation needs no information of true clear image, while PSNR can only be used as criterion of simulated data testing. For a uniform image, ρ equals to zero, and it increases when the difference between image pixels becomes greater. The smaller value of ρ, the higher smoothness of the result. As Table 1 shows, 7 × 1 median filter is the best choice in the lengths varying from 5 to 15. Figure 3(a) is the real IR frame, notice that horizontal stripes are obvious.

Table 1. Roughness Comparison on Original Image and the Corrected Results by Different Filter Lengths

Filter Length	Original	3	5	7
Roughness	0.8423	0.8167	0.8085	0.8023
Filter Length	9	11	13	15
Roughness	0.8057	0.8077	0.8079	0.8083

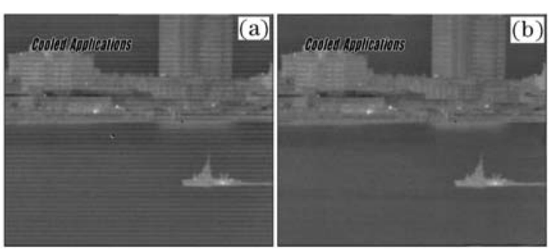

Fig. 3. Correction result of the real IR data.

However in Fig. 3(b), the stripe is completely eliminated. With all small details preserved, the scene of Fig. 3(b) appears uniform.

We presume that the NUC parameters of each detector — gain and offset, are time-varying but remain constant in a block of frames; drift occurs or may become severe between blocks because of the scene changing, which is consistent with the actual operation basically. So in practice, the proposed NUC algorithm can be applied to the first frame of one length-fixed block, getting the correction parameters and using them to compensate nonuniformity for the whole frames of the block. When another block begins, the NUC technique is applied once again and the offset is re-corrected. Such a cycle is repeated as often as necessary during operation of IR FPA.

We have presented an enhanced NNT technique for nonuniformity correction in 1D IR line sensors. A simplified NNT structure is introduced, making the correction parameter update in self-learning process column by column. A vertical median filter is used to smooth horizontal stripes, and the optimal window length can be tested and selected once for all. Furthermore, some optimization techniques are added in order to improve the stability of the algorithm and to accelerate the convergence rate. The final compensators are taken from the mean estimates along rows to reduce ghosting artifacts.

From applications to simulated and real corrupted IR data, it can be concluded that the adaptive NUC algorithm achieves a higher correction level with less complexity. It needs no scene (motion) variation or some statistical assumptions. It can be based on correction between frames and can also be used in intermittent cycles in practical applications, leading to a huge potential for its real-time hardware-based realization.

This work was supported by the Pre-Research Foundation of National Defense under Grant No. 30404. J. Sui's e-mail address is kittysj@gmail.com. W. Jin's e-mail address is jinwq@bit.edu.cn.

References

1. M. M. Hayat, S. N. Torres, E. Armstrong, S. C. Cain, and B. Yasuda, Appl. Opt. **38,** 772 (1999).
2. R. C. Hardie, M. M. Hayat, E. Armstrong, and B. Yasuda, Appl. Opt. **39,** 1241 (2000).
3. B. M. Ratliff, M. M. Hayat, and J. S. Tyo, Proc. SPIE **4820,** 359 (2003).
4. R. A. Leathers, T. V. Downes, and R. G. Priest, Opt. Express **13,** 5136 (2005).
5. D. A. Scribner, K. A. Sarkay, M. R. Kruer, J. T. Caulfield, J. D. Hunt, M. Colbert, and M. Descour, Proc. IEEE **93,** 1955 (1993).
6. S. N. Torres, E. M. Vera, R. A. Reeves, and S. K. Sobarzo, Proc. SPIE **5076,** 130 (2003).